

Additional Insights on the Bastadins: Isolation of Analogues from the Sponge *Ianthella* cf. *reticulata* and Exploration of the Oxime Configurations[†]

Laurent Calcul,[‡] Wayne D. Inman,[‡] Alexi A. Morris,[‡] Karen Tenney,[‡] Joseline Ratnam,[§] James H. McKerrow,[§] Frederick A. Valeriote,[⊥] and Phillip Crews^{*‡}

Department of Chemistry and Biochemistry, University of California, Santa Cruz, California 95064, Sandler Center for Basic Research in Parasitic Disease, University of California, San Francisco, San Francisco, California 94143, and Josephine Ford Cancer Center, Henry Ford Hospital, Detroit, Michigan 48202

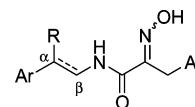
Received September 24, 2009

The focus of this study is on the bastadin class of bromotyrosine derivatives, commonly isolated from *Ianthella* marine sponges, and is the first report on the secondary metabolites from *Ianthella* cf. *reticulata*. Two new bastadins were isolated, (*E,Z*)-bastadin 19 (**1b**), a diastereoisomer of the known (*E,E*)-bastadin 19 (**1a**), and dioxepine bastadin 3 (**2**), an unusual dibenzo-1,3-dioxepine. A bastadin NMR database was created and assisted in the structure determination of **1b** and **2** and the rapid dereplication of 10 other known compounds including bastadins 2–9 (**3–10**), 13 (**11**), and 19 (**1a**). The geometry of the 2-(hydroxyimino)-*N*-alkylamide chains, a chemical feature present in all bastadins, was further probed, and new insights regarding the natural oxime configuration are discussed. Bastadins possessing (*E,Z*)-, (*Z,E*)-, or (*E,E*)-dioxime configurations could be artifacts of isolation or storage in solution. Therefore, this point was explored by photochemical and thermal isomerization studies, as well as molecular mechanics calculations. Bastadins 13 (**11**) and 19 (**1a**) exhibited moderate inhibition against *Trypanosoma brucei*, and bastadin 4 (**5**) was cytotoxic to HCT-116 colon cancer cells.

Sponges of the genus *Ianthella* (order Verongida, family Ianthellidae) produce almost exclusively brominated secondary metabolites. The only exception to this pattern is represented by the bastaxanthin carotenoids.¹ All of the brominated compounds can be divided into two groups: bromobenzofurans represented by the iantherans^{2–4} and bromotyrosine derivatives such as aeropylsin,⁵ ianthelline,⁶ ianthesine,⁷ and the bastadins. The latter group represents the most ubiquitous substances isolated from the genus *Ianthella*. The first examples reported (1980–1981) were from the Verongid sponge *Ianthella basta* and included bastadins 1 and 2 reported by Kazlauskas and co-workers.^{8,9} Subsequently, there have been copious studies on *Ianthella*, resulting in the discovery of some 28 bastadins. Many exhibit cytotoxic activity against cancer cells, and some are still under evaluation as potential therapeutic leads.^{9–16} Somewhat unusual are the additional reports of bastadins from two other sponges including a Verongid of the genus *Psammaphysilla*¹⁵ and the Dendroceratid *Dendrilla*.¹⁶

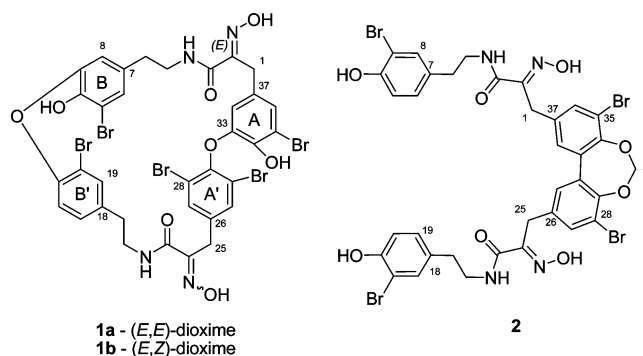
A signature structural feature present in all bastadins reported to date is the (*E*)-2-(hydroxyimino)-*N*-alkylamide functional group (**HI**). The moiety, imbedded in a matrix of bromophenol rings, is also a key residue present in the psammaphin family of bromotyrosines, extensively studied from the Verongida sponge *Pseudoceratina* (aka *Psammaphysilla* or *Druinella*) *purpurea*.¹⁷ Decades ago, Schmitz reported that a psammaphin A diastereomer containing both an (*E*)- and (*Z*)-2-(hydroxyimino)-*N*-alkylamide was transformed on standing to the *E,E* isomer and suggested the *Z,Z* isomer thereof was the natural metabolite that isomerized to *E,E* upon extraction and workup.¹⁸ This significant finding has been overlooked in all subsequent research on bastadin and psammaphin metabolites reported to date.¹⁹

The availability of a recent collection of *I. cf. reticulata* prompted us to reinvestigate the structure of several known bastadins. In this study, we report an isomer of (*E,E*)-bastadin 19 (**1a**) that possesses



HI, R=H or OH

both the (*E*)- and (*Z*)-2-(hydroxyimino)-*N*-alkylamides, which we have named (*E,Z*)-bastadin 19 (**1b**), in addition to the unusual dioxepine bastadin 3 (**2**). The characterization of compound **2**, whose central core, like all bastadins, possessed an H/C ratio < 1,²⁰ was challenging when based on analysis of the NMR data. In order to assist in the structure determination of new analogues and the rapid dereplication of known bastadins, we created a bastadin NMR database that provided benchmark chemical shift values for each aromatic and **HI** substructure found in the bastadins. This database assisted in the structure elucidation of **2**, which contained a dibenzo-1,3-dioxepine group²¹ sandwiched between the two 2-(hydroxyimino)-*N*-alkylamide arrays. Finally, using the bastadin NMR database, we were able to propose ¹H NMR data revisions for bastadin 23.¹⁶



1a - (*E,E*)-dioxime
1b - (*E,Z*)-dioxime

2

Results and Discussion

We examined the methanol extract from *I. cf. reticulata* obtained from Papua New Guinea (coll. no. 05435) by LCMS and concluded it contained a complex mixture of several bastadins. In order to efficiently deal with the vast prior work,

[†] Dedicated to the late Dr. Richard E. Moore of the University of Hawaii at Manoa for his pioneering work on bioactive natural products.

* To whom correspondence should be addressed. Tel: 831-459-2603. Fax: 831-459-2935. E-mail: phil@chemistry.ucsc.edu.

[‡] University of California, Santa Cruz.

[§] Sandler Center BRPD, University of California, San Francisco.

[⊥] Josephine Ford Cancer Center.

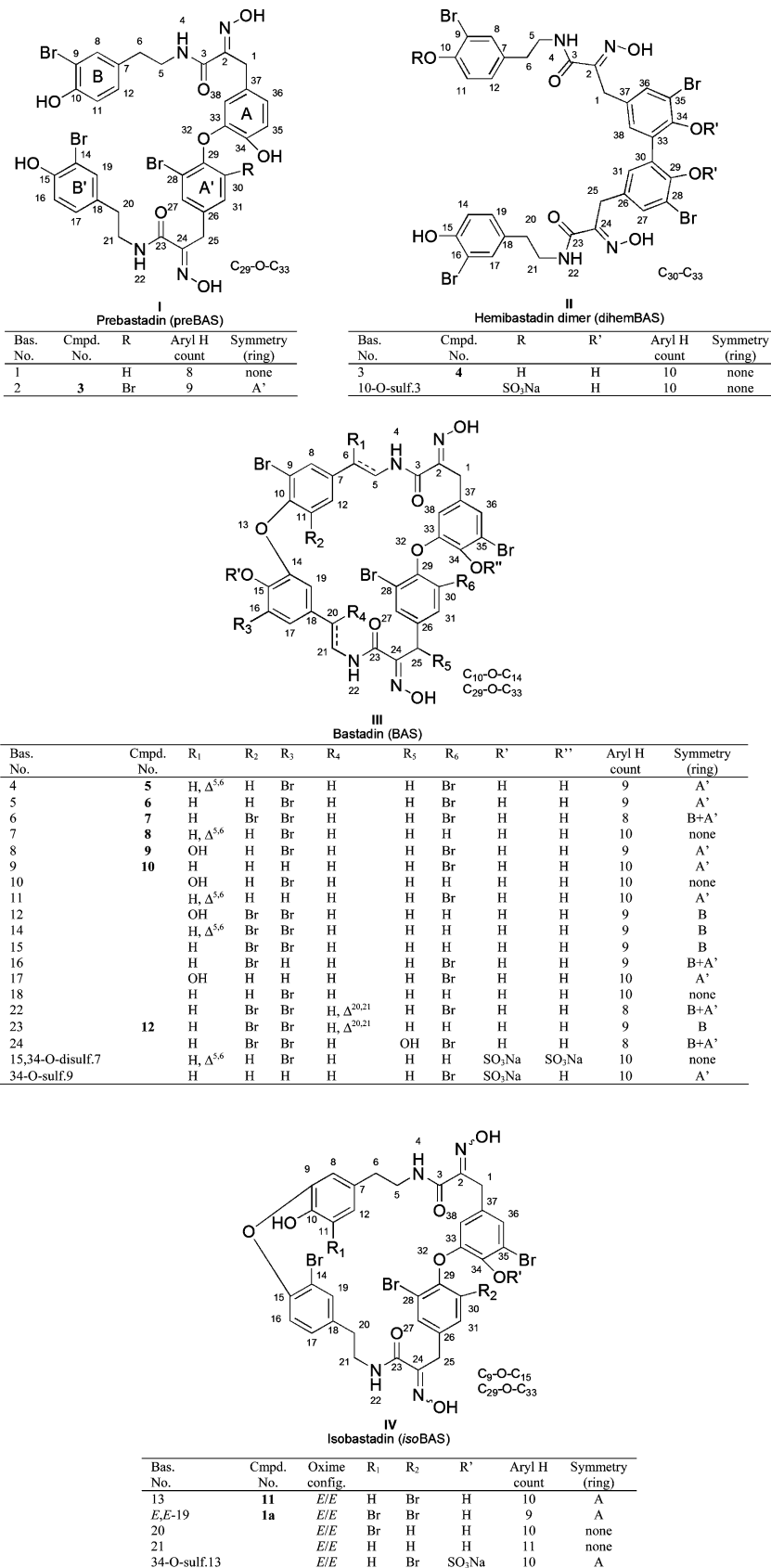


Figure 1. Sponge-derived bastadin structural families consisting of preBAS, dihemBAS, BAS, and isoBAS.

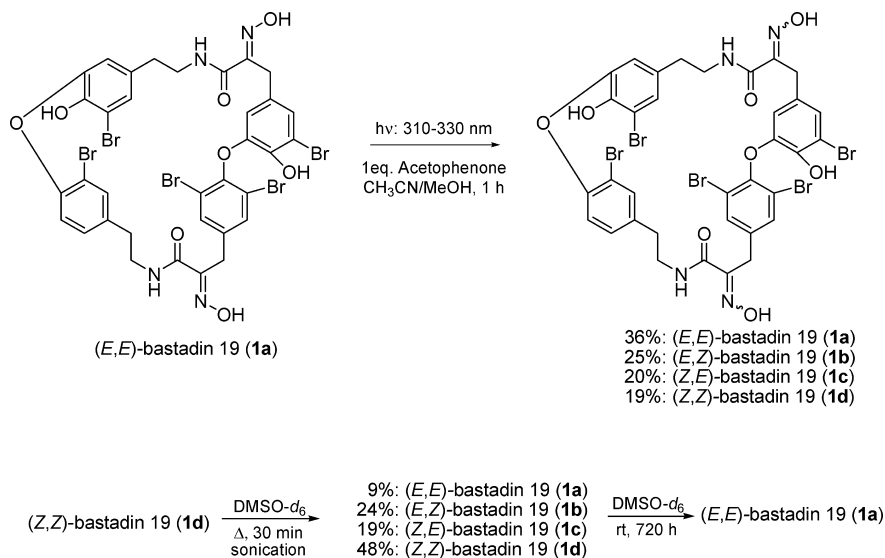
a biogenetically inspired²² outline was assembled, as shown in Figure 1, to include all of the previously reported bastadins. This sketch provided the basis for an immediate dereplication matrix similar to what we previously employed in analyzing sponge-derived oxy-polyhalogenated diphenyl ethers (O-PHDEs).²⁰ The

known bastadins, divided into four structure types, I–IV, based on their aryl–aryl linkages with annotations accompanying each structure, include (1) prebastadin (preBAS, I), (2) dimer of hembastadin (dihemBAS, II), (3) bastadin (BAS, III), and (4) isobastadin (isoBAS, IV).

Table 1. NMR (^1H and ^{13}C in $\text{DMSO}-d_6$) Database Values at Protonated Positions of the Rings and (*E*)-Hydroxyimino-*N*-alkyl Amide Chains from Known Marine Sponge-Derived Bastadins

Rings (A, A', B, B')				<i>(E)</i> -2-(hydroxyimino)- <i>N</i> -alkylamide chains			

^a Values for the presence of two bromines in the aryl at the *ortho* position of the aryl-ether linkage. ^b Values do not include the NMR chemical shifts of bastadin 23. ^c Values for the linkage in α position for $R = 10$. ^d Values for the linkage in α position for $R = 11$. ^e Values for double bond conjugated with a phenol ring. ^f Values for NMR data reported in CD_3CN .

**Figure 2.** Photochemical and thermal interconversions of bastadin 19 (**1a–d**) diastereoisomers.

To employ the information of Figure 1 in dereplicating and recognizing new structures, it is important to note that the bastadin structure is comprised of two classes of constitutional elements. One substructural region contains the four aromatic rings A, B, A', and B' (shown in **I** of Figure 1, with rings coded as 1 to 8 in Table 1), and the other consists of the two **HI** arrays (coded as chains 9 to 12 in Table 1). Easily recognized from Table 1 are that the aryl ring protons exhibit either four distinct ABX systems (first row) or four distinct two-spin systems (second row). Pinpointing the connectivity in the **HI** moiety is straightforward and involves matching data collected to those of either a saturated chain, an unsaturated chain, or two possible saturated chains with an attached OH group. After the rapid identification of the eight possible substructures, collection and analysis of 2D NMR data may be required. Employing the dereplication matrix of Table 1 allowed the characterization of the known bastadins including 2 (**3**),^{8,9} 3 (**4**),⁹ 4 (**5**),^{9,23} 5 (**6**),⁹ 6 (**7**),^{9,14} 7 (**8**),^{9,24} 8 (**9**),^{10,23} 9 (**10**),^{10,23} 13 (**11**),²⁵ and 19 (**1a**).²⁶

The first of the two new metabolites to be analyzed was compound **1b** of formula $\text{C}_{34}\text{H}_{27}\text{Br}_5\text{N}_4\text{O}_8$, as established by HRES-IMS. This formula provided a match to four previously reported bastadins, 5 (**6**),^{9,14,15,22,24,26,27} 15,^{16,28} 16,²⁹ and 19 (**1a**),^{24,26} while also ruling out the presence of benzene rings coded as 3 and 6 in Table 1. The constitutions of the four aryl rings, containing nine protons as three distinct two-spin systems and one ABX pattern, were established using the Table 1 database plus gCOSY NMR data. The specific data (correlated to ring types) included (a) a 2H

singlet at $\delta_{\text{H}} 7.55$ = ring 7, (b) *meta*-coupled protons at $\delta_{\text{H}} 7.15/6.33$ = ring 5, (c) an ABX spin system at $\delta_{\text{H}} 7.50/7.08/6.65$ = ring 4, and (d) a *meta*-coupled system at $\delta_{\text{H}} 6.75/6.01$, which did not match the NMR data of Table 1 but eventually was assigned by 2D NMR data = ring 5. The requirement of such aryl rings ruled out bastadin 16 (comprised of rings = 1, 5, 7, 7). The presence of two nonidentical **HI** residues coded as 9 was approached on the basis of resonances including $\delta_{\text{H}} 2.61$ (t)/2.59 (t); $\delta_{\text{H}} 3.24$ (m)/3.30 (m); and 3.61 (s)/ $\delta_{\text{H}} 3.28$. The two aryl A-**HI**-aryl B and aryl A'-**HI**-aryl B' connectivities determined by gHMBC experiments indicated the **HI** chains were linked as follows: A5-**HI**-B5 and A'7-**HI**-B'4. The mismatch of these arrangements with those of bastadin 5 (**6**) [A5-**HI**-B4 and A'7-**HI**-B'5] and bastadin 15 [A5-**HI**-B7 and A'4-**HI**-B'5] (Figure S2, Supporting Information) ruled out each of these structures. While (*E,E*)-bastadin 19 (**1a**) was consistent with this analysis, it did not fit the C-25 carbon chemical shift ($\delta_{\text{C}} 36.0$) in the southern **HI** group. Schmitz's discussions¹⁸ were the basis for assigning the structure as **1b**, named (*E,Z*)-bastadin 19. This final conclusion was based on using the diagnostic ^{13}C chemical shifts identified for the **HI** oxime allylic methylene: $\delta_{\text{C}} \approx 28$ for the *E* configuration versus $\delta_{\text{C}} \approx 36$ for the *Z* configuration.¹⁸ The relevant ^{13}C NMR data for **1a** are $\delta_{\text{C}} 27.7/28.3$, whereas **1b** exhibits $\delta_{\text{C}} 27.8/36.0$.

At this stage we confirmed that **HI** geometry differences previously observed for two psammaphin A diastereomers were replicated in the bastadin 19 diastereomers **1a** and **1b**. On the basis of this parallel pattern we considered the possibility that all bastadin

Table 2. NMR Data for (*E,E*)-Bastadin 19 (**1a**), (*E,Z*)-Bastadin 19 (**1b**), (*Z,E*)-Bastadin 19 (**1c**), and (*Z,Z*)-Bastadin 19 (**1d**) in DMSO-*d*₆

	1a		1b		1c		1d	
	δ_C	δ_H (J in Hz)	δ_C	δ_H (J in Hz)	δ_C	δ_H (J in Hz)	δ_C	δ_H (J in Hz)
1	27.7	3.38, s	27.8	3.28, s	35.9	3.26, s	35.8	3.16, s
2	151.3		150.8		151.2		150.6	
3	162.9		162.9		161.8		161.5	
4		8.20, t (6.0)		7.75, t (6.8)		8.13, t (6.0)		8.15, brs
5	40.3	3.17, m	39.6 ^a	3.24, m	39.9 ^a	3.13, m	39.9 ^a	3.18, m
6	33.3	2.52, t (7.0)	32.7	2.61, t (6.6)	33.5	2.42, t (6.9)	33.1	2.53, nd
7	131.9		132.1		131.6		131.8	
8	117.6	6.34, d (2.0)	118.4	6.33, d (1.9)	117.7	6.44, d (1.8)	117.8	6.40, brs
9	145.2		144.5		144.9		144.8	
10	143.5		143.9		143.7		143.6	
11	110.9		110.0		110.9		110.9	
12	127.5	7.11, d (2.0)	128.0	7.15, d (1.9)	127.5	7.10, d (1.8)	127.7	7.14, d (1.8)
14	113.4		112.9		113.2		113.0	
15	151.4		151.6		151.2		151.3	
16	120.1	6.78, d (8.0)	119.1	6.65, d (8.7)	119.6	6.83, d (8.4)	119.5	6.79, d (8.4)
17	129.7	7.10, dd (2.0, 8.0)	129.5	7.08, dd (1.9, 8.7)	129.6	7.13, dd (1.8, 8.4)	129.5	7.10, dd (1.8, 8.4)
18	137.0		136.1		137.0		136.5	
19	133.5	7.51, d (2.0)	133.5	7.50, d (1.9)	133.2	7.53, d (1.8)	133.3	7.50, d (1.8)
20	34.0	2.69, t (6.7)	33.9	2.59, t (6.6)	33.1	2.83, t (6.0)	33.4	2.65, t (6.9)
21	39.5 ^a	3.37, m	39.5 ^a	3.30, m	39.4 ^a	3.48, m	39.4 ^a	3.36, m
22		7.79, t (6.0)		8.33, t (6.6)		8.18, t (6.6)		8.32, brs
23	163.2		162.1		163.3		162.4	
24	151.0		151.5		150.9		151.3	
25	28.3	3.73, s	36.0	3.61, s	28.2	3.78, s	35.8	3.57, s
26	137.9		137.3		137.7		137.4	
27	133.1	7.47, s	133.8	7.55, s	133.0	7.47, s	133.7	7.53, s
28	117.3		117.4		117.2		117.2	
29	146.2		146.6		146.2		146.6	
30	117.3		117.4		117.2		117.2	
31	133.1	7.47, s	133.8	7.55, s	133.0	7.47, s	133.7	7.53, s
33	144.6		144.6		143.7		144.5	
34	141.9		141.8		142.2		142.1	
35	110.1		110.1		110.3		110.3	
36	125.9	6.90, d (2.0)	125.1	6.75, d (1.9)	126.8	6.98, d (1.8)	126.5	6.98, d (1.8)
37	128.4		128.4		128.2		128.8	
38	113.0	5.96, d (2.0)	113.2	6.01, d (1.9)	113.2	6.00, d (1.8)	113.0	6.03, d (1.8)
2-NOH		11.95, brs		11.64, brs		12.02, brs		11.58, brs
24-NOH		11.65, brs		11.44, brs		11.44, brs		11.45, brs
10-OH		9.96, brs		9.77, brs		9.81, ^b brs		9.80, brs
34-OH		9.80, brs		9.96, brs		10.00, ^b brs		9.98, brs

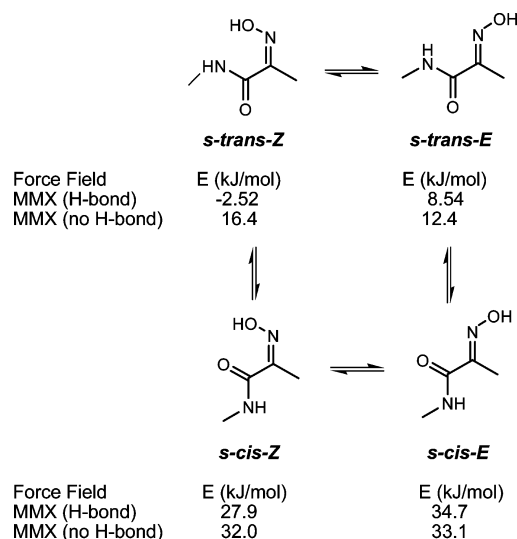
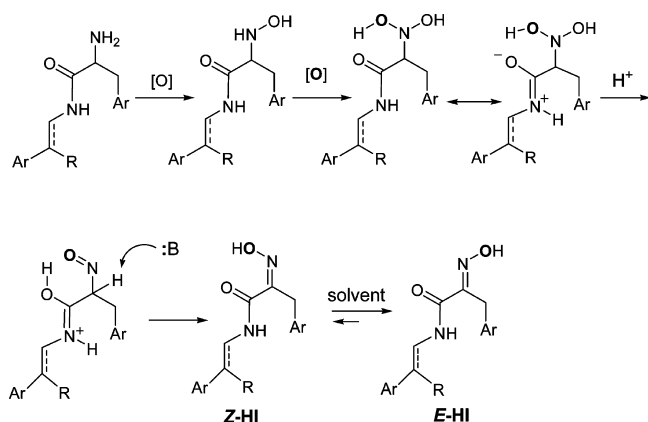
^a Determined by HMBC correlations. ^b Interchangeable signals.

natural products actually contain **HI** moieties with an initial all-*Z* configuration. This intimates that the (*E,Z*), (*Z,E*), or (*E,E*) structures may not be the initial biosynthetic products, but could arise during the isolation steps or during extract storage. Interconversion reactions shown in Figure 2 were conducted to validate this point. First, (*E,E*)-bastadin 19 (**1a**) was subjected to photoisomerization using an incident light of 310–330 nm with acetophenone as triplet sensitizer.³⁰ A mixture of recovered starting material plus new diastereoisomers was obtained consisting of **1a** [*E,E*, 36%], **1b** [*E,Z*, 25%], **1c** [*Z,E*, 20%], and **1d** [*Z,Z*, 19%]. Their geometries were confirmed on the basis of the diagnostic δ_C shifts for C-1/C-25 discussed above and shown in Table 2. Second, the semisynthetic sample of (*Z,Z*)-bastadin 19 (**1d**) was subjected to isomerization in an NMR tube employing heat through brief sonication (30 min). The mixture of diastereoisomers plus starting material obtained consisted of **1a** [*E,E*, 9%], **1b** [*E,Z*, 19%], **1c** [*Z,E*, 24%], and **1d** [*Z,Z*, 48%]. Finally, this mixture of compounds **1a–d**, on standing in solvent for prolonged periods (≈ 720 h) at room temperature, was completely transformed into **1a**.

The configurational lability of (*E*)- and (*Z*)-oximes has been previously explored. Oximes in the solid state display a high degree of configurational stability; however equilibrium between the *E* and *Z* isomers occurs in solution, and the thermodynamically favored isomer predominates.³¹ In order to gain additional insights for the configurational stability of the **HI** residue in solution, molecular mechanics calculations were carried out on (*E*)- and (*Z*)-2-

(hydroxyimino)-*N*-methylpropanamide as a simplified model. We wanted to compare the calculated results with our solution observations described above. Molecular mechanics calculations began with a conformation search in Spartan '06, resulting in four global minima being predicted, *s-trans-Z*, *s-cis-Z*, *s-trans-E*, and *s-cis-E*, whose structures are shown in Scheme 1. Two possible conformations, *s-trans* and *s-cis*, exist for each *E* and *Z* configurational isomer. The minimized energies, with and without H-bonding, for each of the four isomers were calculated with the MMX force field (dielectric constant = 1.5) in PCMODEL and are shown in Scheme 1. Both sets of calculations with and without H-bonding predict that the *s-cis* conformations are at least 15 kJ/mol higher than the corresponding *s-trans*, indicating a negligible population of any *s-cis* conformer at room temperature in solution. The lowest energy among the *s-trans* isomers with H-bonding was calculated for *s-trans-Z* (−2.52 kJ/mol), which has a H-bond between the hydrogen of the amide N–H and oxygen of the oxime (1.72 Å). However, without this intramolecular H-bond the *s-trans-E* calculated energy is lower than *s-trans-Z* by 4.0 kJ/mol, and the former would predominate in solution. The latter case more closely reflects the results we observed, where intramolecular H-bonding is minimized due to solvation, and **1b**, **1c**, and **1d** undergo thermal isomerization to **1a** in solution.

The occurrence of the (*Z*)-oxime functional group is rare in natural products. In plants, the tyrosine-derived glucosinolate and cyanogenic glucoside dhurrin involve the transformation of L-

Scheme 1. Calculated Global Energy Minima of (*E*)- and (*Z*)-2-(Hydroxyimino)-*N*-methylpropanamides**Scheme 2.** Extension of Townsend's (*Z*)-Oxime Biosynthetic Proposal³⁴ to Rationalize the Initial Biosynthesis of **Z-HI** in Bastadins and Psammaplins Followed by *Z*-*E* Isomerization in Solution

tyrosine to (*Z*)-*p*-hydroxyphenylacetaldehyde oxime.³² Nocardicin A, a novel β -lactam from the actinomycete *Nocardia uniformis*, contains a 2-(hydroxyimino)-*N*-alkylamide substructure strikingly similar to those found in bastadins. Biosynthetic studies have suggested that the oxidation of the amine to (*Z*)-oxime in nocardicin A may proceed through a similar mechanism to that proposed for dhurrin.³³ An intramolecular hydrogen-bonding mechanism was proposed to account for the predominant formation of (*Z*)-oxime (nocardicin A) relative to (*E*)-oxime (nocardicin B).³⁴ This mechanism aptly accounts for the biosynthesis of (*Z*)-oximes in bastadin **1b** and psammaplins (Scheme 2), as well as the preferential formation of (*E*)-*p*-hydroxyphenylacetaldehyde oxime over the (*Z*)-oxime in dhurrin. Two successive oxidations of the amine lead to a *N,N*-dihydroxy-**HI** intermediate in which one of the hydroxyls is hydrogen bonded to the neighboring amide, fixing the position of the two oxygen atoms and precluding the free rotation about the C–N bond. This intermediate is supported by observations in dhurrin biosynthetic studies that have shown the *N*-hydroxylation reactions are catalyzed by a multifunctional monooxygenase with a single catalytic site where the second oxygen incorporated in the *N*-hydroxytyrosine is quantitatively retained in the *p*-hydroxyphenylacetaldehyde oxime (the second oxygen is denoted as bold in Scheme 2).³⁵ The neighboring amide facilitates dehydration to form the nitroso-**HI** intermediate and then tautomerization leading to the (*Z*)-oxime. On the basis of these biosynthetic studies, Schmitz's *E*-*Z* isomerization results, and in our current work, we are tempted

Table 3. NMR Data for Bastadin 3 (**4**) and Dioxepine Bastadin 3 (**2**) in DMSO-*d*₆

position	4		2	
	δ_C	δ_H (J in Hz)	δ_C	δ_H (J in Hz)
1, 25	27.6	3.71, s	28.3	3.83, s
2, 24	151.7		151.3	
3, 23	162.9		163.0	
4, 22		7.93, t (6.6)		8.02, t (6.6)
5, 21	40.4	3.29, m	40.3	3.30, m
6, 20	33.6	2.63, t (7.4)	33.5	2.64, t (6.6)
7, 18	131.4		131.5	
8, 17	132.5	7.28, d (1.9)	132.6	7.28, d (1.9)
9, 16	108.9		109.0	
10, 15	152.2		152.3	
11, 14	116.2	6.82, d (8.3)	116.2	6.83, d (8.7)
12, 19	128.7	6.95, dd (1.9, 8.3)	128.8	6.96, dd (1.9, 8.7)
26, 37	128.9		135.8	
27, 36	132.0	7.30, d (1.9)	132.8	7.51, d (1.9)
28, 35	111.2		115.4	
29, 34	149.6		147.7	
30, 33	127.6		132.6	
31, 38	131.0	6.94, d (1.9)	128.5	7.40, d (1.9)
39			101.3	5.66, s
2/24-NOH		11.79, brs		11.97, brs
9/15-OH		10.01, brs		9.99, brs
29/34-OH		8.95, brs		

to speculate that all bastadin and psammaplins metabolites are produced with the (*Z*)-oxime configuration and subsequently isomerize to the more thermodynamically favored *E* isomer in solution.

The next substance analyzed, compound **2**, displayed a HREIMS *m/z* at $[M - H]^-$ 952.8664 for the formula C₃₅H₂₉Br₄N₄O₈ and is unique in the bastadin family. A symmetrical dimeric biaryl-containing structure, analogous to that of bastadin 3 (**4**) [C₃₄H₃₀Br₄N₄O₈],^{9,23} was intimated from the count of H₁₅ and C₁₈ observed by NMR. These two compounds had parallel NMR properties, as shown in Table 3. The aryl and aliphatic groups present were pinpointed from ¹H and HMQC NMR data including (a) an ABX spin system, δ_H 7.28/6.83/6.96 = ring 2 for two aryl groups (Table 1); (b) a *meta*-coupled constellation at δ_H 7.51/7.40, for two aryl rings not represented in Table 1; (c) **HI** arrays identified as chain 9 by the methylene protons at δ_H 3.30; δ_H 2.64 and δ_H 3.83 (Table 1); and (d) an isolated dioxy-methylene at δ_H 5.66 (2H, s), δ_C 101.3. The gHMBC correlations from H-27/H-36 and H-31/H-38 to C-1/C-25 provided conclusive evidence that the two identical side chains were attached to the biaryl ring at C-26/C-37 of **2**. This connection was also supported by NOESY correlations from δ_H 3.83 (H-1/H-25) to δ_H 7.40 (H-31/H-38) and to δ_H 7.51 (H-27/H-36). Finally, gHMBC correlations from H₂-39 at δ_H 5.66 to δ_C 147.7 (C-29/C-34) and also from H-27/36 and H-31/38 to C-29/C-34 linked the biaryl system through the isolated methylene at C-39. These 2D NMR data sets required embedding a 1,3-dioxepine ring into the biaryl system to complete the structure, which we named dioxepine bastadin 3 (**2**). The dibenzo-1,3-dioxepine scaffold is rare in natural products chemistry and is found only in the cercosporins isolated from *Cercospora* spp., a terrestrial fungus.³⁶ We do not consider this compound to be an artifact generated during the isolation process from possible diol condensation with methylene chloride or other solvents.

During the dereplication process we discovered that the aryl ¹H NMR data reported in the literature for bastadin 23 (**12**)¹⁶ did not match the patterns expected based on the trends shown in Table 1. Of further concern was that its structure was based solely on 1D ¹H NMR analysis and 2D NOESY correlations. The literature values shown in Figure 3, especially for δ_H 6.58 (H-27), are not in accord with an aryl H-27 proton *ortho* to the Br and *meta* to an OAr, which is the substitution pattern of ring A' (Figure S3, Supporting Information) of structure **12**. There are two possibilities for revisions to rectify this ambiguity (Figure 3). One involves the amended

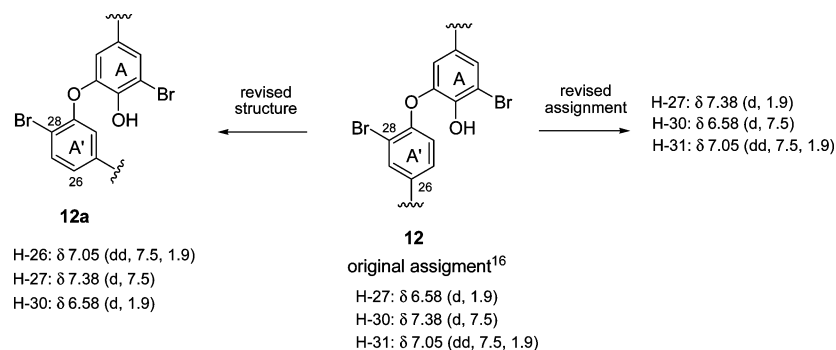


Figure 3. Literature ^1H NMR assignment¹⁶ for the A' ring in bastadin 23 (**12**) and possible revisions.

Table 4. Distribution of Bastadins Reported in this Study within Marine Sponges

bas. no.	cmpd. No.	<i>Ianthella basta</i>	<i>Ianthella quadrangulata</i>	<i>Ianthella flabelliformis</i>	<i>Dendrilla cactos</i>	<i>Psammaplysilla purpurea</i>
2	3	•8,9		•22		
3	4	•9,24				
4	5	•8,9,24,26	•14			
5	6	•9,22,24,26,27	•14	•22,38a		•15
6	7	•9,22,24	•14	•38a	•16	
7	8	•9,24,26	•14		•16	•15
8	9	•10,23				
9	10	•10,23		•38a		
13	11	•25	•14	•38a		
19	1a	•26		•38b	•16	

^a Comparison of exact mass measurements with literature data indicated the presence of bastadins 5, 6, 9, 10, and 11 or corresponding isomeric bastadins 12, 13, 15, 16, 18, and 20.^{38, b} This reference failed to mention that bastadin 19 cannot easily be distinguished using exact mass measurements from bastadins 5, 15, and 16.³⁸

assignments shown for structure **12**, and it incorporates the assumption that literature J values are misreported. The other requires a revised structure **12a** whose ring A' provides an acceptable rationalization of the observed ^1H NMR data. We preferred the first option because the substitution pattern of ring A' in **12a** is inconsistent with both all prior bastadin structures and the overview of the biogenetic pathways²¹ leading to its members.

The bioassay component of this project included evaluation of both extract fractions and pure compounds. The MeOH extract (coded XFM) showed 80% inhibition at 1.25 $\mu\text{g}/\text{mL}$ against *T. brucei*, the causative agent of human African trypanosomiasis (sleeping sickness), designated as a neglected tropical disease (NTD) by the National Institutes of Health.³⁷ Several compounds including **1a**, **1b**, **2**, **3**, and **5–11** were evaluated against the parasite. This follow-up screening revealed that only the *isoBAS*-type structure with its ether linkages $\text{C}_9\text{--O--C}_{15}$ and $\text{C}_{29}\text{--O--C}_{33}$ (Figure 1) such as bastadin 13 (**11**) [$\text{IC}_{50} = 1.77 \mu\text{M}$] and bastadin 19 (**1a**) [$\text{IC}_{50} = 1.31 \mu\text{M}$] exhibited significant inhibition against *T. brucei*, although the testing set did not include the dioxepine bastadin 3 (**2**), due to its scarcity, nor the three isobastadins (**1b–1d**) due to their instability. Additional screening involved evaluation of **1a**, **1b**, **2**, and **4–7** against the colon carcinoma cell line HCT-116. Among this set, only bastadin 4 (**5**) [$\text{IC}_{50} = 1.28 \mu\text{M}$] showed significant activity.

Conclusions

The most consistent sources of the bastadins are sponges from the genera *Ianthella* (order Verongida, family Ianthellidae). The results reported in our isolation work underscore this point, and the sponge *Ianthella cf. reticulata* represents, as shown in Table 4, a fourth such species containing these heteroatom-rich structures. The literature also clearly shows (Table 4) that the bastadins can be isolated from other sponges identified as *Psammaplysilla*¹⁵ (order Verongida, family Aplysinnellidae) and *Dendrilla*¹⁶ (order Dendroceratida, family Darwinellidae). However, for each of the two non-*Ianthella* sponges there is only one report of bastadins (*D. cactos* and *P. purpurea*). Consequently, these results seem inconsistent

and could be explained by errors in establishing their identity. It is tempting to envision that the bastadin bromotyrosine family represents a chemical signature for the genus *Ianthella*. Our isolation of (*E,Z*)-bastadin 19 (**1b**) is significant and points to the difficulty of obtaining bastadin analogues of all-*Z* geometry. On the basis of our photochemical and thermal isomerization results, molecular mechanics calculations of a **HI** analogue, and reported biosynthetic studies, we propose the bastadins and psammaplins initially contain the (*Z*)-oxime configuration and subsequently isomerize to the more thermodynamically stable *E* isomer in solution during extraction and/or workup. Another unexpected finding of this study was the isolation of **2**, a new dibenzo-1,3-dioxepine derivative of the known bastadin 3 (**4**). The bastadin database assembled here will facilitate future studies of bastadin-containing sponges, whose structures are challenging to establish because a core element has an H/C ratio of less than 1.

Experimental Section

General Experimental Procedures. The NMR spectra were recorded in DMSO- d_6 , acetone- d_6 , and CD_3OD on a Varian 500 and 600 MHz for ^1H and at 125 MHz for ^{13}C NMR. High- and low-resolution mass measurements were obtained respectively from a FAB and an ESI-TOF mass spectrometer. LCMS were performed with a Phenomenex Luna C₁₈ RP 5 μm column (150 \times 4.6 mm) using an ESITOFMS, a Waters 996 photodiode array detector, and a Sedex55 evaporative light scattering (ELS) detector. Semipreparative HPLC was performed using a Phenomenex 5 μm Luna C₁₈ RP column (250 \times 10 mm) by using a single wavelength ($\lambda = 254 \text{ nm}$) for compound detection.

NMR Database and Calculations. The bastadin NMR database was generated by averaging chemical shift values within each substructure type from reported literature values; see Supporting Information, Figures S1–S4, for individual chemical shifts. Chemical shifts were averaged, and the error was reported to three standard deviations. Molecular modeling was carried out with Spartan '06, version 1.1.2, Wavefunction Inc., June 15, 2007. Global minima were calculated using the Conformer Distribution program in Spartan '06 utilizing the SYBYL force field. Energy minimization was carried out with PCMODEL, version 7.5

(Serena Software), using the MMX force field, Steepest Descent minimization method, dielectric constant = 1.5, with and without H-bonds.

Animal Material. The sponge (coll. no. 05435, 500 g wet weight) was collected in November 2005 by scuba in Milne Bay (10°37.005' S, 150°95.620' E), Papua New Guinea. Collection depth was approximately 30 ft. The sponge was identified taxonomically by Dr. Nicole J. de Voogd as *I. cf. reticulata*, and a voucher specimen was deposited at the Naturalis, National Museum of Natural History, Leiden, The Netherlands, under the registration number RMNH Por 5392.

Extraction and Isolation. Samples were preserved in the field according to our standard laboratory procedures³⁹ and stored at 4 °C until extraction was performed. The sponges were extracted with hexanes (XFH), CH₂Cl₂ (XFD), and MeOH (XFM) using an accelerated solvent extractor (ASE). The MeOH extract (05435XFM, >1 g) was submitted to a H₂O-*n*-BuOH partitioning procedure. The resultant *n*-BuOH-soluble extract (05435XFMWBS, 850 mg) was fractionated using several rounds of semipreparative reversed-phase HPLC (flow rate: 2 mL/min). Isocratic conditions were employed with CH₃CN and water, each containing 0.1% formic acid. The fractionation (54:46 CH₃CN-H₂O) afforded 23 fractions. Fractions H4 (55.3 mg, 6.1 × 10⁻²% dry weight), H6 (106.0 mg, 1.2 × 10⁻¹% dry weight), H8 (28.7 mg, 3.2 × 10⁻²% dry weight), H16 (120.0 mg, 1.3 × 10⁻¹% dry weight), and H18 (18.2 mg, 2.0 × 10⁻²% dry weight) provided **4**, **11**, **9**, **1a**, and **8**, respectively. Fractions H7 (23.0 mg), H9 (23.0 mg), H12 (4.6 mg), H20 (23.0 mg used of 37.2 mg), and H22 (11.7 mg) were each purified using 45:55 CH₃CN-H₂O and gave, respectively, **3** (4.0 mg, 4.0 × 10⁻³% dry weight), **10** (2.4 mg, 3.0 × 10⁻³% dry weight), **1b** (2.0 mg, 2.0 × 10⁻³% dry weight), **5** (11.0 mg, 1.2 × 10⁻²% dry weight) accompanied by **6** (3.5 mg, 4.0 × 10⁻³% dry weight), and **7** (2.0 mg, 2.0 × 10⁻³% dry weight) accompanied by **2** (1.1 mg, 1.0 × 10⁻³% dry weight).

Sensitized Photoisomerization. A degassed solution containing acetophenone (triplet sensitizer) and **1a** (30 nM) in 1 mL of acetonitrile-methanol (3:1) was irradiated through one Pyrex culture tube at 310–330 nm for 2 h. The resultant residue was fractionated using semipreparative reversed-phase HPLC with acetonitrile and water (52:48 CH₃CN-H₂O), each containing 0.1% formic acid. Fractions H2 (4.5 mg, 19% yield), H4 (6.6 mg, 20% yield), H6 (8.6 mg, 25% yield), and H8 (11.3 mg, 36% yield) provided **1d**, **1c**, **1b**, and **1a**, respectively.

Thermal Isomerization. A solution of **1d** in DMSO-*d*₆ contained in a NMR tube was sonicated in a beaker of MeOH for 30 min. The resultant ¹H NMR spectrum is available as Figure S23 (Supporting Information).

Room-Temperature Isomerization. The mixture of **1a–d** obtained from the thermal isomerization of **1d** (see above) in DMSO-*d*₆ was kept at room temperature for 720 h.

Cytotoxicity against HCT-116. IC₅₀ values were determined as previously described.⁴⁰

Trypanosoma brucei Assay. IC₅₀ values were determined as previously described.³⁷

(E,E)-Bastadin 19 (1a): white powder; ¹H NMR and ¹³C NMR in DMSO-*d*₆ (see Table 2); ESIMS [M - H]⁻ *m/z* 1012.8 (11), 1014.8 (56), 1016.8 (100), 1018.8 (99), 1020.8 (56), 1022.8 (13).

(E,Z)-Bastadin 19 (1b): white powder; ¹H NMR and ¹³C NMR in DMSO-*d*₆ (see Table 2); ESIMS [M - H]⁻ *m/z* 1012.5 (6), 1014.5 (55), 1016.5 (99), 1018.5 (100), 1020.5 (38), 1022.5 (3); HRESIMS [M - H]⁻ *m/z* 1012.7677 (calcd for C₃₅H₂₉⁷⁹Br₄N₄O₈ 1012.7668).

(Z,E)-Bastadin 19 (1c): white powder; ¹H NMR and ¹³C NMR in DMSO-*d*₆ (see Table 2); ESIMS [M - H]⁻ *m/z* 1012.5 (6), 1014.5 (55), 1016.5 (99), 1018.5 (100), 1020.5 (38), 1022.5 (3).

(Z,Z)-Bastadin 19 (1d): white powder; ¹H NMR and ¹³C NMR in DMSO-*d*₆ (see Table 2); ESIMS [M - H]⁻ *m/z* 1012.5 (6), 1014.5 (55), 1016.5 (99), 1018.5 (100), 1020.5 (38), 1022.5 (3).

Dioxepine bastadin 3 (2): white powder; ¹H NMR and ¹³C NMR in DMSO-*d*₆ (see Table 3); ESIMS [M - H]⁻ *m/z* 948.9 (7), 606.6 (46), 608.6 (100), 610.6 (89), 612.6 (51), 614.6 (11); HRESIMS [M - H]⁻ *m/z* 948.8714 (calcd for C₃₅H₂₉⁷⁹Br₄N₄O₈ 948.8724).

Bastadin 2 (3): white powder; NMR data are in accordance with the literature.⁹

Bastadin 3 (4): white powder; ¹H NMR and ¹³C NMR in DMSO-*d*₆ (see Table 3); ¹H NMR (CD₃OD, 600 MHz) δ_H 7.42 (2H, d, *J* = 1.8 Hz, H-27/36), 7.30 (2H, *J* = 1.8 Hz, H-8/17), 7.06 (2H, d, *J* = 1.8 Hz, H-31/38), 6.96 (2H, dd, *J* = 1.8, 8.1 Hz, H-12/19), 6.78 (2H, d, *J* = 8.1 Hz, H-11/14), 3.84 (4H, s, H-1/25), 3.38 (4H, t, 7.2, H-5/21),

2.67 (4H, t, 6.6, H-6/20); ¹³C NMR (CD₃OD, 125 MHz) δ_C 165.9 (C-3/23), 153.9 (C-10/15), 153.2 (C-2/24), 150.9 (C-29/34), 134.4 (C-8/17), 134.1 (C-27/36), 133.2 (C-7/18), 132.8 (C-31/38), 131.3 (C-26/37), 130.2 (C-12/19), 128.8 (C-30/33), 117.4 (C-11/14), 112.6 (C-28/35), 110.9 (C-9/16), 42.2 (C-5/21), 35.4 (C-6/20), 28.9 (C-1/25); ESIMS [M - H]⁻ *m/z* 1014.7 (6), 1016.7 (55), 1018.7 (97), 1020.7 (100), 1022.7 (41), 1024.7 (11).

Bastadin 4 (5): white powder; NMR data are in accordance with the literature.²³

Bastadin 5 (6): white powder; NMR data are in accordance with the literature.⁴¹

Bastadin 6 (7): white powder; NMR data are in accordance with the literature.^{9,16}

Bastadin 7 (8): white powder; NMR data are in accordance with the literature.²⁴

Bastadin 8 (9): white powder; [α]_D²⁵ -2.8 (c 1, MeOH); NMR data are in accordance with the literature.²⁵

Bastadin 9 (10): white powder; NMR data are in accordance with the literature.²³

Bastadin 13 (11): white powder; NMR data are in accordance with the literature.²⁵

Acknowledgment. This research was supported by NIH grant R01-CA047135 (P.C.) and NMR equipment grants from NSF CHE-0342912 and NIH S10-RR19918. We thank W. Boggess at the University of Notre Dame for providing HRESIMS measurements and R. Bogomolni at the University of California Santa Cruz for use of the lamp to perform the photoisomerization reaction. We would like to thank L. Matainaho, University of Papua New Guinea, and the crew and skipper (C. DeWit) of the *M/V Golden Dawn* for assistance in specimen collection.

Note Added after ASAP Publication: This paper was published on the Web on Jan 26, 2010, with an error in Table 3. The corrected version was reposted on Feb 25, 2010.

Supporting Information Available: Tables and figures are provided that include mass spectrometry and NMR spectroscopy studies for **1b–d**, **2**, and **4**. This material is available free of charge via the Internet at <http://pubs.acs.org>.

References and Notes

- Ramdahl, T.; Kazlauskas, R.; Bergquist, P.; Liaajensen, S. *Biochem. Syst. Ecol.* **1981**, *9*, 211–213.
- Okamoto, Y.; Ojika, M.; Sakagami, Y. *Tetrahedron Lett.* **1999**, *40*, 507–510.
- Okamoto, Y.; Ojika, M.; Suzuki, S.; Murakami, M.; Sakagami, Y. *Bioorg. Med. Chem.* **2001**, *9*, 179–183.
- Greve, H.; Meis, S.; Kassack, M. U.; Kehraus, S.; Krick, A.; Wright, A. D.; Konig, G. M. *J. Med. Chem.* **2007**, *50*, 5600–5607.
- Minale, L.; Sodano, G.; Chan, W. R.; Chen, A. M. *J. Chem. Soc., Chem. Commun.* **1972**, 674–675.
- Litaudon, M.; Guyot, M. *Tetrahedron Lett.* **1986**, *27*, 4455–4456.
- Okamoto, Y.; Ojika, M.; Kato, S.; Sakagami, Y. *Tetrahedron* **2000**, *56*, 5813–5818.
- Kazlauskas, R.; Lidgard, R. O.; Murphy, P. T.; Wells, R. J. *Tetrahedron Lett.* **1980**, *21*, 2277–2280.
- Kazlauskas, R.; Lidgard, R. O.; Murphy, P. T.; Wells, R. J.; Blount, J. F. *Aust. J. Chem.* **1981**, *34*, 765–786.
- Miao, S.; Andersen, R. J. *J. Nat. Prod.* **1990**, *53*, 1441–1446.
- Pettit, G. R.; Butler, M. S.; Bass, C. G.; Doubek, D. L.; Williams, M. D.; Schmidt, J. M.; Pettit, R. K.; Hooper, J. N. A.; Tackett, L. P.; Filiatrault, M. J. *J. Nat. Prod.* **1995**, *58*, 680–688.
- Aoki, S.; Cho, S.; Hiramatsu, A.; Kotoku, N.; Kobayashi, M. *J. Nat. Med.* **2006**, *60*, 231–235.
- Aoki, S.; Cho, S.; Ono, M.; Kuwano, T.; Nakao, S.; Kuwano, M.; Nakagawa, S.; Gao, J. Q.; Mayumi, T.; Shibuya, M.; Kobayashi, M. *Anticancer Drugs* **2006**, *17*, 269–278.
- Greve, H.; Kehraus, S.; Krick, A.; Keller, G.; Maier, A.; Fiebig, H. H.; Wright, A. D.; Konig, G. M. *J. Nat. Prod.* **2008**, *71*, 309–312.
- Carney, J. R.; Scheuer, P. J.; Kelly-Borges, M. *J. Nat. Prod.* **1993**, *56*, 153–157.
- Reddy, A. V.; Ravinder, K.; Narasimhulu, M.; Sridevi, A.; Satyanarayana, N.; Kondapi, A. K.; Venkateswarlu, Y. *Bioorg. Med. Chem.* **2006**, *14*, 4452–4457.
- Piña, I. C.; Gautschi, J. T.; Wang, G. Y.; Sanders, M. L.; Schmitz, F. J.; France, D.; Cornell-Kennon, S.; Sambucetti, L. C.; Remiszewski, S. W.; Perez, L. B.; Bair, K. W.; Crews, P. *J. Org. Chem.* **2003**, *68*, 3866–3873.

- (18) Arabshahi, L.; Schmitz, F. J. *J. Org. Chem.* **1987**, *52*, 3584–3586.
- (19) Fusetani, N.; Masuda, Y.; Nakao, Y.; Matsunaga, S.; van Soest, R. W. M. *Tetrahedron* **2001**, *57*, 7507–7511 Tokaradines A and B were reported as the (*Z*)-oxime isomer; however we believe the authors incorrectly assigned the configuration. The *E* geometry would more aptly account for the *syn*-methylene carbon chemical shift of 30.7 ppm.
- (20) Calcul, L.; Chow, R.; Oliver, A. G.; Tenney, K.; White, K. N.; Wood, A. W.; Fiorilla, C.; Crews, P. *J. Nat. Prod.* **2009**, *72*, 443–449.
- (21) Keana, J. F. W.; Morse, R. H. *Tetrahedron Lett.* **1976**, 2113–2114.
- (22) Jaspars, M.; Rali, T.; Laney, M.; Schatzman, R. C.; Diaz, M. C.; Schmitz, F. J.; Pordesimo, E. O.; Crews, P. *Tetrahedron* **1994**, *50*, 7367–7374.
- (23) Pordesimo, E. O.; Schmitz, F. J. *J. Org. Chem.* **1990**, *55*, 4704–4709.
- (24) Franklin, M. A.; Penn, S. G.; Lebrilla, C. B.; Lam, T. H.; Pessah, I. N.; Molinski, T. F. *J. Nat. Prod.* **1996**, *59*, 1121–1127.
- (25) Butler, M. S.; Lim, T. K.; Capon, R. J.; Hammond, L. S. *Aust. J. Chem.* **1991**, *44*, 287–296.
- (26) Mack, M. M.; Molinski, T. F.; Buck, E. D.; Pessah, I. N. *J. Biol. Chem.* **1994**, *269*, 23236–23249.
- (27) Masuno, M. N. H., A. C.; Pessah, I. N.; Molinski, T. F. *Mar. Drugs* **2004**, *2*, 176–184.
- (28) Dexter, A. F.; Garson, M. J.; Hemling, M. E. *J. Nat. Prod.* **1993**, *56*, 782–786.
- (29) Sun Ku, P.; Jurek, J.; Carney, J. R.; Scheuer, P. J. *J. Nat. Prod.* **1994**, *57*, 407–410.
- (30) Padwa, A.; Albrecht, F. *J. Am. Chem. Soc.* **1974**, *96*, 4849–4857.
- (31) Tennant, G. In *Comprehensive Organic Chemistry, The Synthesis and Reaction of Organic Compounds*; Barton, D., Ollis, W. D., Eds.; Pergamon Press: Oxford, 1979; Vol. 2, Part 8, pp 383–590.
- (32) Sibbesen, O.; Koch, B.; Halkier, B. A.; Moller, B. L. *J. Biol. Chem.* **1995**, *270*, 3506–3511.
- (33) Kelly, W. L.; Townsend, C. A. *J. Am. Chem. Soc.* **2002**, *124*, 8186–8187.
- (34) Kelly, W. L.; Townsend, C. A. *J. Bacteriol.* **2005**, 739–746.
- (35) Halkier, B. A.; Lykkesfeldt, J.; Moller, B. L. *Proc. Natl. Acad. Sci. U.S.A.* **1991**, *88*, 487–491.
- (36) Lousberg, R. J. J. Ch.; Weiss, U.; Salemink, C. A.; Amone, A.; Merlini, L.; Nasini, G. *Chem. Commun.* **1971**, 1463–1464.
- (37) Rubio, B. K.; Tenney, K.; Ang, K. H.; Abdulla, M.; Arkin, M.; McKerrow, J. H.; Crews, P. *J. Nat. Prod.* **2009**, *72*, 218–222.
- (38) Motti, C. A.; Freckelton, M. L.; Tapiolas, D. M.; Willis, R. H. *J. Nat. Prod.* **2009**, *72*, 290–294.
- (39) Rodriguez, J.; Nieto, R. M.; Crews, P. *J. Nat. Prod.* **1993**, *56*, 2034–2040.
- (40) Robinson, S. J.; Tenney, K.; Yee, D. F.; Martinez, L.; Media, J. E.; Valeriote, F. A.; van Soest, R. W. M.; Crews, P. *J. Nat. Prod.* **2007**, *70*, 1002–1009.
- (41) Couladouros, E. A.; Pitsinos, E. N.; Moutsos, V. I.; Sarakinos, G. *Chem. Eur. J.* **2001**, *11*, 406–421.

NP9005986